DIRECT NUMERICAL SIMULATION OF SURFACE BLOCKING EFFECTS ON ISOTROPIC AND AXISYMMETRIC TURBULENCE

Kouji Nagata
Department of Mechanical Science and Engineering,
Nagoya University
Nagoya 464-8603, Japan
nagata@nagoya-u.jp

Peter. A. Davidson
Department of Engineering,
University of Cambridge
Cambridge CB2 1PZ, UK
pad3@eng.cam.ac.uk

Julian. C. R. Hunt
Department of Earth Science,
University College London
London WC1E 6BT, UK
julian.hunt@cpom.ucl.ac.uk

Yasuhiko Sakai
Department of Mechanical Science and Engineering,
Nagoya University
Nagoya 464-8603, Japan
ysakai@mech.nagoya-u.ac.jp

Satoru Komori
Department of Mechanical Engineering and Science,
and Advanced Research Institute of Fluid Science and Engineering,
Kyoto University
Kyoto 606-8501, Japan
Komori@mech.kyoto-u.ac.jp

INTRODUCTION

In turbulent flows near rigid surfaces the fluctuating velocity field is either generated locally by mean velocity gradients and body forces or transported there by the mean flow and self induced motions of the eddies (e.g. Högström *et al.* 2002). However, the structure of turbulence is also influenced by the kinematic conditions at the surface, i.e., the parallel and normal components of the velocity should be zero or match those of the surface (Hunt and Graham 1978). In turbulent shear-free flows such as thermal convection (e.g. Hunt 1984), turbulence near an air-water interface (e.g. Komori *et al.* 1993; Pan and Banerjee 1995) and a sharp density interface (e.g. Kit *et al.* 1997) they are essential in determining the eddy structures and other properties of the flow.

In this paper we present the results of direct numerical simulations (DNS) of isotropic and axisymmetric anisotropic turbulence impinging onto a planar surface, which have been analysed using the rapid distortion theory (RDT) by Nagata *et al.* (2006). The present DNS is also an extension of Perot and Moin (1995) to an anisotropic turbulence using an alternative forcing technique based on Townsend's 'simple model eddies' (Townsend 1976). The results are compared with the RDT analysis (Nagata *et al.* 2006).

DIRECT NUMERICAL SIMULATION

A forcing method has been used to generate stationary, homogeneous and isotropic/axisymmetric turbulence. The force field is obtained in real space by sprinkling many localised 'blobs' of forcing whose centres are randomly but uniformly distributed in space. In a cylindrical coordinate (r,θ,z), the force field associated with a spherical blob of forcing orientated along the axis Oz is represented by

$$F_{eddy} = \Omega^2 r \exp\left\{-\frac{2\left(r^2+z^2\right)}{le^2}\right\}\mathbf{e}_\theta, \quad (1)$$

where Ω^2 is the amplitude of forcing, l_e is the characteristic length scale of the blob and $\mathbf{e}_\theta$ is the angular unit vector. Each blob exerts a localised torque, but no net linear force, to the fluid. This provides a random forcing, yet retains phase coherence. The axes of torque are in random directions for generating an isotropic turbulence and are aligned for generating an axisymmetric anisotropic turbulence (Fig.1). For the axisymmetric turbulence, the axis of symmetry (of axisymmetric turbulence) is set to lie on the x-y plane and the angle is $\alpha = \pi/4$ from the x-axis, which is typical in the atmospheric surface layer. F_x', F_y' and F_z' in Fig.1 are the average forces aligned to the axis of anisotropy, x', y', z'. By using different model blobs of different sizes and intensities and by controlling the axes of torque, stationary homogeneous isotropic and axisymmetric anisotropic turbulences with various turbulent Reynolds numbers are obtained.

The governing equations for DNS to generate the turbulent field with forcing are

$$\frac{\partial u_i}{\partial x_i} = 0, \quad (2)$$

$$\frac{\partial u_i}{\partial t} + u_j\frac{\partial u_i}{\partial x_j} = -\frac{1}{\rho}\frac{\partial p}{\partial x_i} + \nu\frac{\partial^2 u_i}{\partial x_j \partial x_j} + F_i, \quad (3)$$

where,

$$\mathbf{F} = \left(F_x, F_y, F_z\right) = \sum_{i=1}^{N_{eddy}} \mathbf{F}_{eddy,i}. \quad (4)$$

Note that the force field satisfies the solenoidal condition. The MAC (Marker and Cell) method based on the finite difference method was used to solve the N-S equations. The computational domain is a box with side length L and height $1.2L$. The number of grid points is $129(x)\times151(y)\times129(z)$. First, slip conditions are applied to all the boundaries to generate stationary, homogeneous isotropic/axisymmetric turbulence. Then, at $t_w = 0$, a flat surface is inserted at y=0 in the fully developed flow and the non-slip condition is applied to the surface. The initial velocities and pressure are zero, so that no initial turbulent (or random) field has to be specified in the present method. The super computer NEC SX-6 at the Center for Global Environmental Research, National Institute for Environmental Studies, Environmental Agency of Japan was used.

RESULTS AND DISCUSSION

Stationary, Homogeneous and Isotropic Turbulence without the Surface Blocking

Time developments of the turbulence intensities and the correlation coefficients of the Reynolds stresses are shown in Figs. 2 and 3 for $\mathrm{Re}_L = u_\infty' L_\infty/\nu = 40$, where u_∞' is the rms velocity free from the wall (or in the fully developed flow before the wall-insertion) and L_∞ is the streamwise

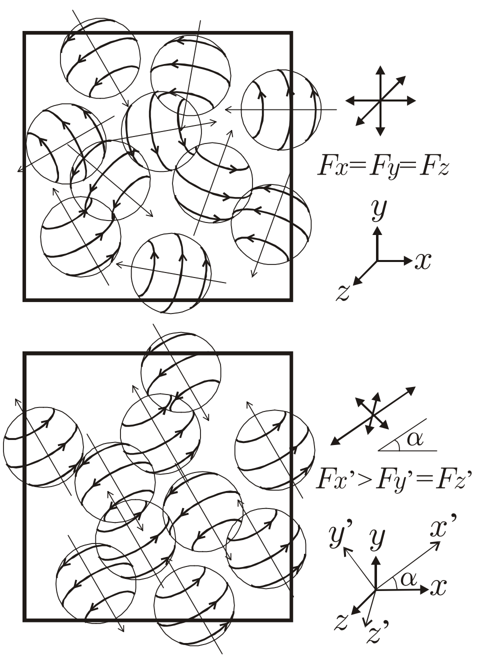

Figure 1: Sketch of the arrangements of forcing blobs: upper: for generating an isotropic turbulence; lower: for generating an axisymmetric turbulence.

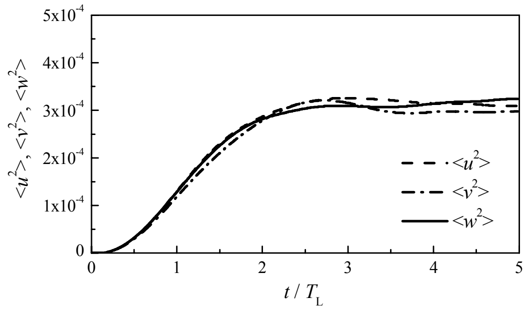

Figure 2: Time developments of the turbulence intensities of velocity fluctuations at $\mathrm{Re}_L = 40$.

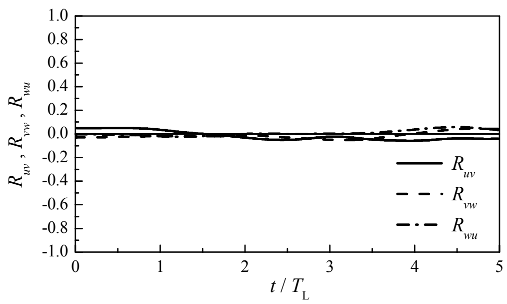

Figure 3: Time developments of the Reynolds stresses at $\mathrm{Re}_L = 40$.

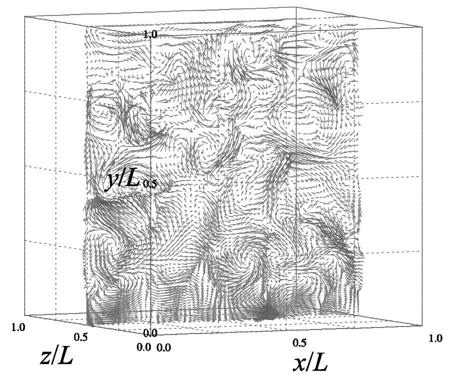

Figure 4: A typical velocity field over the flat wall.

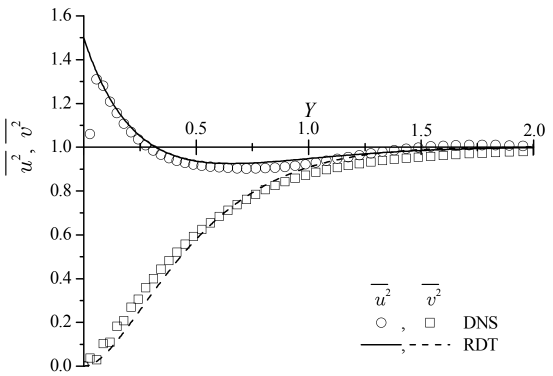

Figure 5: The vertical distributions of the turbulence intensities at $t_w / T_L = 0.01$ at $\mathrm{Re}_L = 80$.

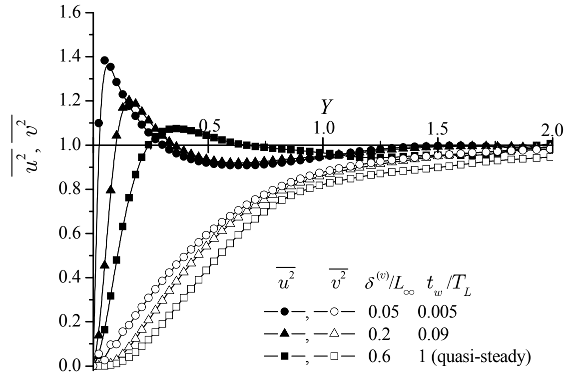

Figure 6: The vertical distributions of the turbulence intensities at $\mathrm{Re}_L = 40$. $\delta^{(v)}$ is the thickness of viscous layer (Hunt and Graham 1978).

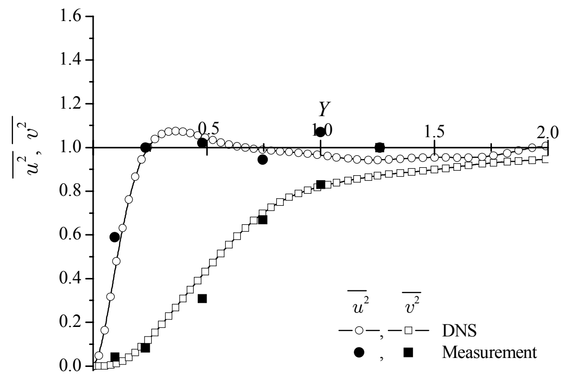

Figure 7: The vertical distributions of the turbulence intensities at the quasi steady state at $\mathrm{Re}_L = 40$.

integral length scale free from the wall. < > denotes the space-average and the time is normalised by the eddy turnover time of the developed flow, $T_L = L_\infty / u_\infty'$. It is found from Fig.2 that the fully developed flow is attained after $t / T_L \geq 3$. The turbulence intensities are almost identical (the maximum ratio of the turbulence intensities between two different components is less than 1.1) and the Reynolds stress is very small (the absolute values of the correlation coefficients are less than 0.05). The results show that the fully developed, stationary, isotropic field is generated using the present method. Similar results were obtained for different Reynolds numbers.

Surface Blocking of Isotropic Turbulence

Figure 4 shows the typical velocity field over the flat wall at $t_w / T_L = 0.01$. Due to the non-slip condition at the wall, now the velocity components are zero at y=0, which causes the blocking effects. Figure 5 shows the vertical distributions of the turbulence intensities at $\mathrm{Re}_L = 80$ and at $t_w / T_L = 0.01$. Overbar denotes the time-average and the vertical distance from the wall y is normalised by L_∞, i.e., $Y = y / L_\infty$. Also shown in the figure are the turbulence intensities obtained by the RDT analysis (Nagata *et al.* 2006). The result of the DNS agrees quite well with the RDT and so-called the splat effect (i.e., turbulence intensities of the components parallel to the surface are amplified; see Hunt and Graham 1978 for detail) is noticeable near the wall. The result also suggests the validity of both the present DNS and previous RDT. Note the difference between the DNS and RDT in the vicinity of the surface. $\overline{u^2}$ obtained by the DNS decreases in the vicinity of the surface because of the viscous effect (i.e., the nonslip condition). In the RDT, the limiting value at the surface has the non-zero value of 3/2 because of the inviscid analysis. However, the effect of the viscosity is found to be confined to a very thin layer for relatively high Reynolds numbers and the RDT can predict the overall feature of the turbulence quantities in the shear-free turbulent boundary layer.

Figure 6 shows the time variation of turbulence intensities at $\mathrm{Re}_L = 40$. The Reynolds number for this case is the same as that in the previous measurement in the mixing box by McDougall (1979). At small t_w, the splat effect occurs near the wall. However, as t_w increases, the viscous effect attenuates the splat effect. The same tendency was observed even at higher Reynolds number of $\mathrm{Re}_L = 80$. The result is qualitatively agrees with Perot and

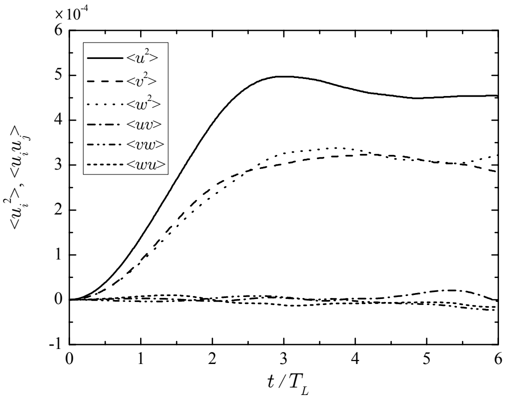

Figure 8: Time developments of the turbulence intensities and Reynolds stress at $\mathrm{Re}_L = 80$.

Moin (1995). Figure 7 compares the result of the DNS ($\mathrm{Re}_L = 40$) in the quasi-steady state with the measurements of McDougall (1979). There is good agreement between the measurements and the DNS. The results confirm that, at low Reynolds numbers ($\mathrm{Re}_L = O(10^2)$), the splat effect occurs only after a short time following the surface insertion (or near the leading edge of moving-wall downstream of turbulence-generating grid (e.g. Uzkan and Reynolds 1967)) and the steady splat effect cannot be generated.

Stationary, Homogeneous and Axisymmetric Turbulence without the Surface Blocking

Time developments of the turbulence intensities and Reynolds stresses are shown in Fig. 8 for $\mathrm{Re}_L = 80$. Here *u*, *v* and *w* are the turbulent components parallel (*u*) and perpendicular (*v* and *w*) to the principal axis of the axisymmetric turbulence. It is found that the fully developed flow is attained after $t / T_L \geq 4$. The Reynolds stresses are very small and $\langle u^2 \rangle > \langle v^2 \rangle \cong \langle w^2 \rangle$. The results show that fully developed, stationary, axisymmetric anisotropic turbulence is created using the present method. Similar results were obtained for different Reynolds numbers. The ratio of the turbulence intensities *R* is approximately 1.5 (in Fig.8), which is typical in the atmospheric turbulent boundary layer. Note that *R* can be adjusted by the arrangement of the forcing-blobs.

Surface Blocking of Axisymmetric Turbulence

Figure 9 shows the vertical distributions of turbulence intensities at $\mathrm{Re}_L = 80$ and at $t_w / T_L = 0.01$ together with the RDT analysis. The splat effect occurs near the surface as in the isotropic case. The streamwise and vertical components of the turbulence intensities, $\overline{u^2}$ and $\overline{v^2}$, show excellent agreements with the RDT. The agreement of spanwise component $\overline{w^2}$ is acceptable, with a maximum difference of 13% between the DNS and RDT. The results suggests the validity of the present DNS and the previous RDT using the ansats of Sreenivasan and Narasimha (1978) to define the three-dimensional energy spectrum tensor. The

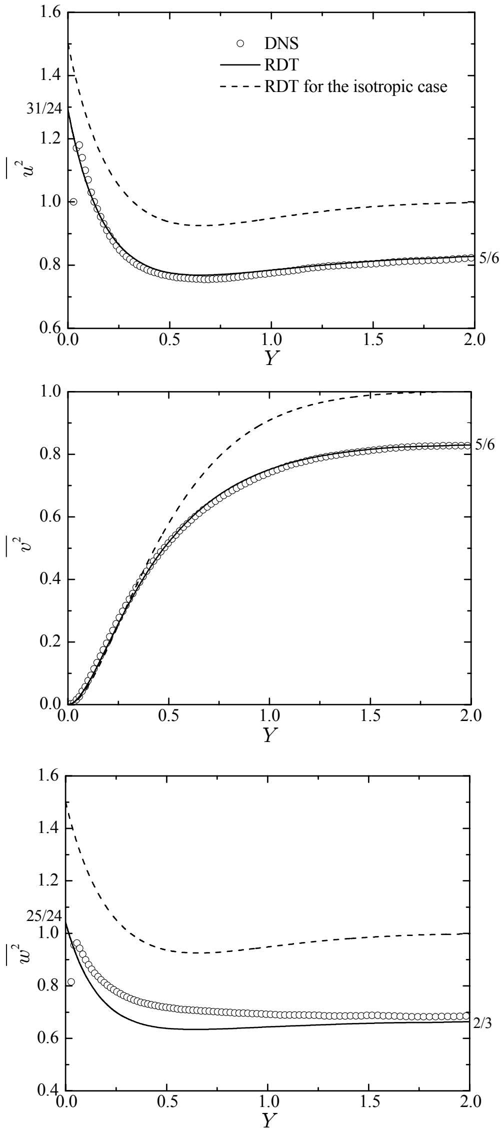

Figure 9: The vertical distributions of the turbulence intensities for the blocking of *axisymmetric* turbulence at $\mathrm{Re}_L = 80$ and at $t_w / T_L = 0.01$.

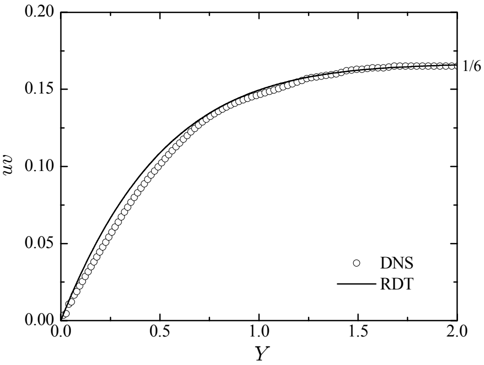

Figure 10: The vertical distribution of the Reynolds stress at $\mathrm{Re}_L = 80$ and at $t_w / T_L = 0.01$.

difference of spanwise intensity between the DNS and RDT may be due to the nonlinear transfer of turbulence energy from vertical to spanwise direction, which is not included in the RDT.

Figure 10 shows the vertical distribution of the Reynolds stress. The result agrees well with the RDT analysis. It is found that the profile of Reynolds stress hardly changes with time (not shown here). Due to the gradients of Reynolds stress near a planar surface, an initially shear free flow might become a sheared turbulent flow (Nagata *et al*., 2006). In the present DNS, however, we did not observe the mean flow generation by the blocking of axisymmetric turbulence because the Reynolds number is not high. The results qualitatively agree with the previous measurement in a mixing box (Wong 1985), in which the mean motion was observed only when the frequency of the oscillating-grid is over 7Hz (i.e., when the Reynolds number is sufficiently high).

CONCLUSIONS

The direct numerical simulations (DNS) of isotropic and axisymmetric anisotropic turbulence impinging onto a planer surface are conducted and the results are compared with the previous RDT analysis. The main results from this study are as follows.

1. Stationary, homogeneous and isotropic/axisymmetric turbulence can be generated in real space using the present method. By using different model blobs of different sizes and intensities and by controlling the axes of torque, stationary homogeneous isotropic and axisymmetric anisotropic turbulences with various turbulent Reynolds numbers are obtained.
2. The turbulence intensities near the wall, influenced by the surface blocking of isotropic/axisymmetric turbulence, showed good agreements with the previous measurement and the rapid distortion theory (RDT) analysis.

ACKNOWLEDGEMENTS

The authors would like to thank Mr. Fumihiko Sagara for his help in this study. The direct numerical simulations were carried out by using the supercomputer NEC SX-6 at the Center for Global Environmental Research, National Institute for Environmental Studies, Environmental Agency of Japan. This study was partially supported by the Japanese Ministry of Education, Culture, Sports, Science and Technology through Grants-in-Aid (No.18686015) and the Center of Excellence for Research and Education on Complex Functional Mechanical Systems (COE program of the Ministry of Education, Culture, Sports, Science and Technology, Japan).

REFERENCES

Högström, U.L.F., Hunt, J.C.R. and Smedman, A.S., 2002, “Theory and Measurements for Turbulence Spectra and Variances in the Atmospheric Neutral Surface Layer,” Boundary-Layer Meteorology., Vol. 103, pp. 101-124.

Hunt, J.C.R. and Graham, J.M.R. 1978, “Free-Stream Turbulence Near Plane Boundaries,” Journal of Fluid Mechanics, Vol. 84, pp.209-235.

Hunt, J.C.R., 1984, “Turbulence Structure in Thermal Convection and Shear-Free Boundary Layers,” Journal of Fluid Mechanics, Vol. 138, pp.161-184.

Kit, E.L.G., Strang, E.J. and Fernando, H.J.S., 1997, “Measurement of Turbulence Near Shear-Free Density Interfaces,” Journal of Fluid Mechanics, Vol. 334, pp. 293-314.

Komori, S. *et al.*, 1993, “Direct Numerical Simulation of Three-Dimensional Open-Channel Flow with Zero-Shear Gas-Liquid Interface,” Physics of Fluids A, Vol. 5, No.1, pp. 115-125.

McDougall, T.J., 1979, “Measurements of Turbulence in a Zero-Mean-Shear Mixed Layer,” Journal of Fluid Mechanics, Vol. 94, pp. 409-431.

Nagata, K., Wong, H., Hunt, J.C.R., Sajjadi, S.G. and Davidson, P.A., 2006, “Weak Mean Flows Induced by Anisotropic Turbulence Impinging onto Planar and Undulating Surfaces,” Journal of Fluid Mechanics, Vol. 556, pp. 329-360.

Pan, Y. and Banerjee, S., 1995, “A Numerical Study of Free-Surface Turbulence in Channel Flow,” Physics of Fluids, Vol. 7, No. 7, pp. 1649-1664.

Perot, B. and Moin, P., 1995, “Shear-Free Turbulent Boundary Layers. Part 1. Physical Insights into Near-Wall Turbulence,” Journal of Fluid Mechanics, Vol. 295, pp. 199-227.

Sreenivasan, K.R. and Narasimha, R., 1978, “Rapid Distortion of Axisymmetric Turbulence,” Journal of Fluid Mechanics, Vol. 84, pp. 497-516.

Townsend, A.A., 1976, The Structure of Turbulent Shear Flow, Cambridge Univ. Press.

Uzkan , T. and Reynolds, W. C., 1967, “A shear-free turbulent boundary layer,” Journal of Fluid Mechanics, Vol. 28, pp. 803-821.

Wong, H.Y.W., 1985, “Shear-Free Turbulence and Secondary Flow near Angled and Curved Surfaces,” PhD Thesis, University of Cambridge.